Metal-Organic Frameworks Based on Halogen-bridged Dinuclear-Cu-nodes as Promising Materials for High Performance Supercapacitor Electrodes

Xin Xiong,[a] Liuyin Zhou,[a] Wenjie Cao,[a] Jiyuan Liang,[a] Yazheng Wang,[a] Siqian Hu[a], Fan Yu,[a,*] and Bao Li[b]

Materials and General Methods

The organic ligand HL and other reagents for the syntheses were of analytical grade and used as received from commercial sources without further purification. Elemental analyses (C, H and N) were determined on a Perkin-Elmer 2400 analyzer. The IR spectra were recorded as KBr pellets on a Nicolet Avatar-360 spectrometer in the 4000-400 cm^{-1} region. Thermogravimetric analysis (TGA) was performed on a Perkin-Elmer TG-7 analyzer heated from 25 to 700 ℃ under nitrogen atmosphere. Powder X-ray diffraction (PXRD) patterns for the as-synthesized samples were recorded on a X-ray diffraction meter (D/max 2500 PC, Rigaku) with Cu-*K*α radiation (1.5406 Å).

Synthesis of $\{[Cu_2ClH_2O(L)_2]\cdot(CH_3OH)_4\}_n$ (1)

A mixture of CuCl(5mg) and HL(10mg) were dissolved in 5 mL of CH_3OH, and pH of the resulted solution was adjusted to 7. The reaction mixture was sonicated for 5 minutes before heated in the 130℃ isothermal oven for 2 days. Blue crystal sample was obtained in yield of 55%. EA result for $C_{36}H_{37}ClCu_2N_6O_9$: Calcd (%):C, 50.26%, H, 4.34%, N, 9.77%; found C, 50.98%, H, 4.09%, N, 10.32%. IR(KBr,cm^{-1}): 3421, 1613, 1546, 1391, 1307, 1257, 1218, 1056, 844, 788.

Synthesis of $\{[Cu_2BrH_2O(L)_2]\cdot(CH_3OH)_4\}_n$ (2).

A mixture of CuBr(5mg) and HL(10mg) were dissolved in 5 mL of CH_3OH , and pH of the resulted solution was adjusted to 7. The reaction mixture was sonicated for 5 minutes before heated in the 130℃ isothermal oven for 2 days. Blue crystal sample

was obtained in yield of 40%. EA result for $C_{36}H_{37}BrCu_2N_6O_9$: Calcd (%):C, 47.79%, H, 4.12%, N, 9.29%; found C, 48.17%, H, 3.92%, N, 9.55%. IR(KBr,cm^{-1}): 3420, 1614, 1546, 1391, 1307, 1218, 1056, 844, 788.

Synthesis of $\{[Cu(H_2O)(L)_2]\cdot(H_2O)\}_n$ (3).

A mixture of CuI(5mg) and HL(10mg) were dissolved in 6 mL H_2O/0.2 mL dioxane. The reaction mixture was sonicated for 5 minutes before heated in the 85℃ isothermal oven for 2 days. Blue crystal sample was obtained in yield of 25%. EA result for $C_{32}H_{24}CuN_6O_6$: Calcd (%):C, 58.94%, H, 3.71%, N, 12.89%; found C, 58.57%, H, 3.44%, N, 13.35%. IR(KBr,cm^{-1}): 3418, 1613, 1543, 1392, 1306, 1215, 1054, 843, 788.

Single crystal X-ray diffraction

X-ray diffraction data of **1** - **3** were collected via Bruker APEX-II CCD diffractometer using Cu-*Kα* (λ = 1.54178 Å) and Mo-*Kα* (λ = 0.71073 Å) radiation. The structures of complexes were solved by direct methods, and the non-hydrogen atoms were located from the trial structure and then refined anisotropically with SHELXTL using a full-matrix least squares procedure based on F^2 values. The *PLATON/SQUEEZE* routine was employed to calculate the diffraction contribution from the solvent molecules, and thereby to produce a set of solvent-free diffraction intensities. According to the results of EA and TGA, four methanol molecules have been squeezed for each formula. The hydrogen atom positions were fixed geometrically at calculated distances and allowed to ride on the parent atoms. CCDC-1560294, 1560295 and 1581237 for **1-3** contain the supplementary crystallographic data for this paper. These data can be obtained free of charge from The Cambridge Crystallographic Data Centre. A summary of the structural determination and refinement for compound **1** and **2** is listed in Table 1.

Electrochemical measurements

The working electrode was fabricated by the following procedure. The Cu-based MOFs, acetylene black, and poly(tetrafluoroethylene) were mixed in a mass ratio of 80 : 10: 10 and dispersed in ethanol to produce a homogeneous paste. Acetylene black

and poly(tetrafluoroethylene) were used as the conductive agent and the binder. The slurry was coated on a nickel foam substrate (1 cm × 1 cm) and dried at 60 °C for 8 h under vacuum. The as-formed electrode was then pressed at 10 MPa and further dried at 100 °C for 6 h. All electrochemical characterizations were evaluated using a CHI660E electrochemical workstation (Chenhua Instrument Co. Ltd., Shanghai, China), and a 6 M potassium hydroxide aqueous solution as an electrolyte with a three-electrode configuration at room temperature. The as-prepared nickel foam-based electrode was used as the working electrode, and the detailed electrode fabrication was described above. The platinum wire and Hg/HgO electrodes were employed as the counter and reference electrodes, respectively. Cyclic voltammograms (CV) were recorded within the range of 0 to 0.6 V at various scan rates. Galvanostatic charge-discharge (GCD) curves were obtained in the same potential range at different current densities. Moreover, the long-term cycle stability of the working electrode was determined by the GCD measurement at a current density of 1 A g^{-1}.

Table S1. the comparison of supercapacitive properties of reported pristine MOFs materials utilized as active electrode materials

Sample	Electrolyte	Supercapacitor	Cycling Performances
Co-MOF[1]	5M KOH	2564 Fg^{-1} at 1 F g^{-1}	95.8% after 3000 times
Ni-MOF[2]	6M KOH	1127 Fg^{-1} at 0.5 A g^{-1}	90% after 3000 times
Co-MOF film[3]	1M LiOH	206.7 Fg^{-1} at 0.5 A g^{-1}	98.5% after 3000 times
Ni-MOF [4]	2M KOH	552 Fg^{-1} at 1 A g^{-1}	98% after 3000 times
Zr-MOF_1[5]	6M KOH	1144 Fg^{-1} at 0.5 A g^{-1}	---
Cu-MOF@C[6]	6M KOH	138 Fg^{-1} at 0.5 A g^{-1}	86% after 2000 times
Cu-LCP[7]	1M LiOH	1102 Fg^{-1} at 1 A g^{-1}	88% after 2000 times

*[1] Chem. Eur.J.2017, 23,631;[2] J. Mater. Chem. A, 2014, 2, 16640;[3] Microporous and Mesoporous Materials 2012,153,163;[4] Nano Energy 2016, 26, 66;[5] RSC Adv., 2015, 5, 17601;[6] Inorg. Chem. 2016, 55, 6552; [7] Dalton Trans., 2015, 44, 19175

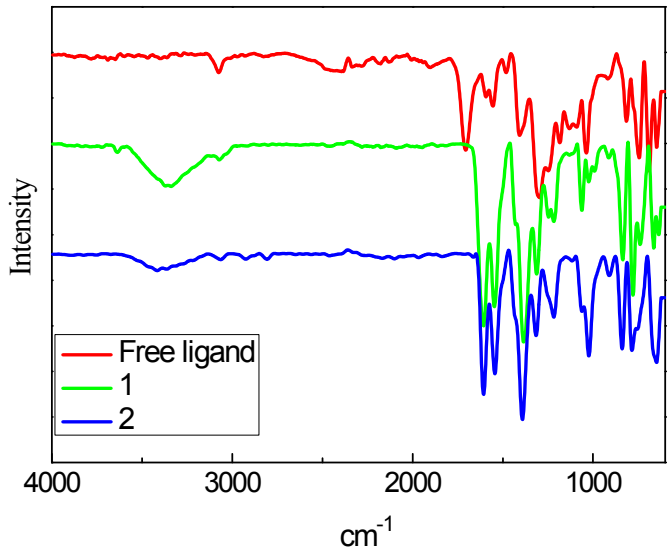

Figure S1. IR spectra of free ligand, 1 and 2

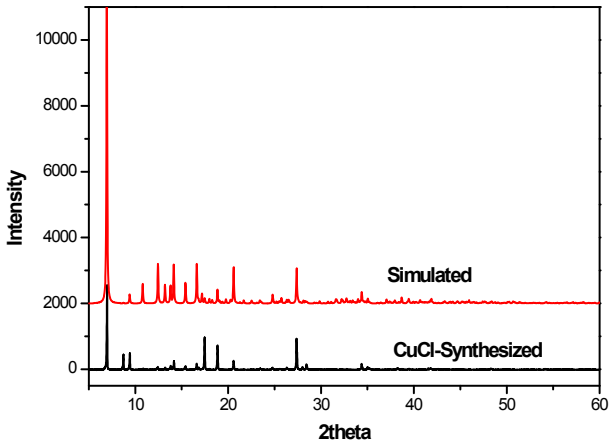

Figure S2. XRD spectra of 1

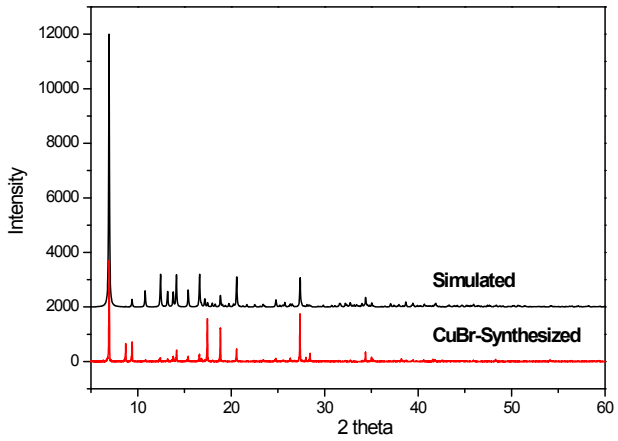

Figure S3. XRD spectra of 2

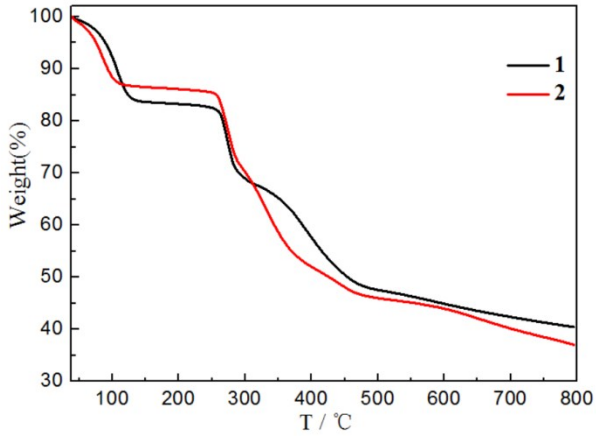

Figure S4. TGA curve of 1 and 2

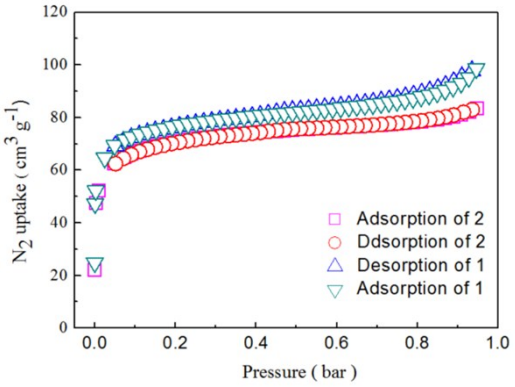

Figure S5. The sorption isotherms of N_2 of **1** and **2**. Blue triangle and red cirlce, N_2 desorption; green triangle and purple square, N_2 adsorption.

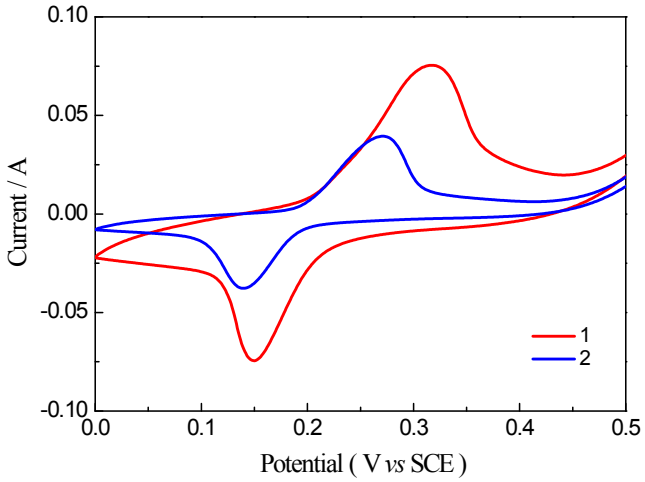

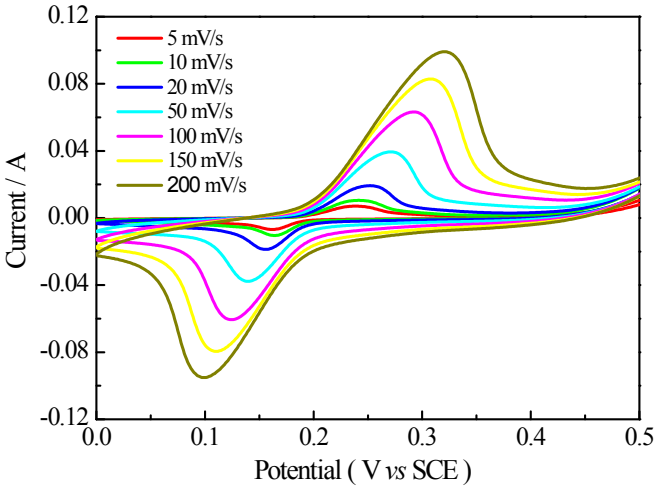

Figure S6. (up)Cyclic voltammogram curves of **1** and **2** electrodes at 50 mV s^{-1} .(down) Cyclic voltammogram curves of **2** electrode at different scan rates in the range of 5-200 mV s^{-1} .

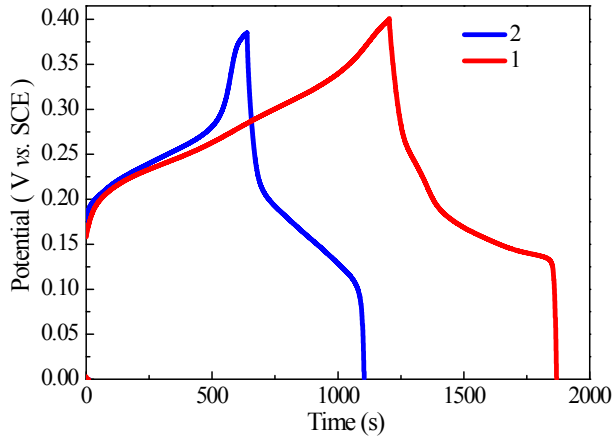

Figure S7. The galvanostatic charge-discharge curves of **1** and **2** electrodes at current densities of 0.5 A g^{-1} in 6 M potassium hydroxide aqueous solution.

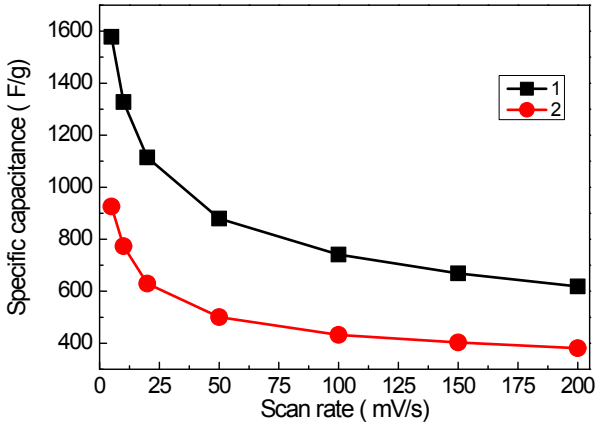

Figure S8. Specific capacitances of **1** and **2** electrodes derived from the discharging curves at the different scan rate in 6 M potassium hydroxide aqueous solution;

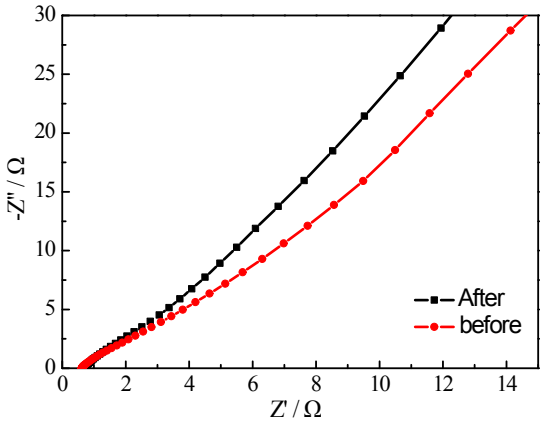

Figure S9. EIS plots of **1** electrode before and after the long cycling test (2000 cycles).

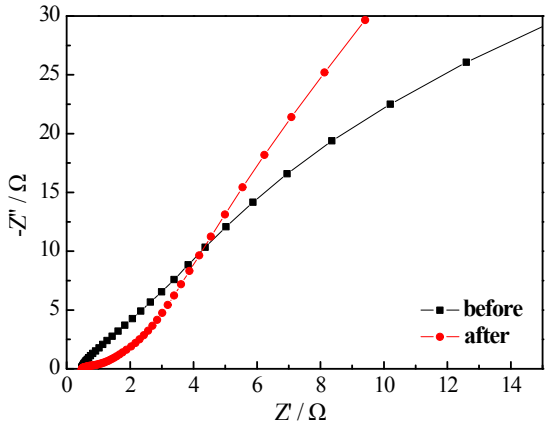

Figure S10. EIS plots of **2** electrode before and after the long cycling test (2000 cycles).

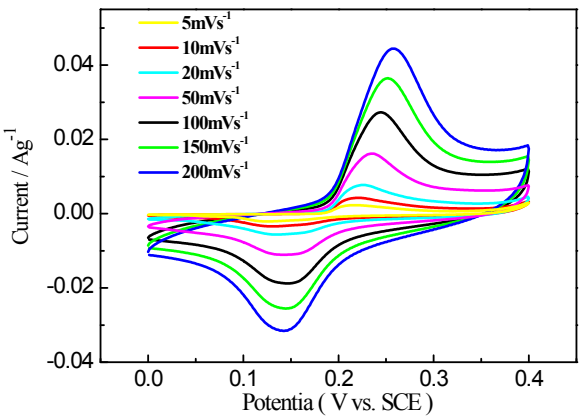

Figure S11. Cyclic voltammogram curves of **1** electrode at different scan rates in the range of 5-200 mV s^{-1} ..

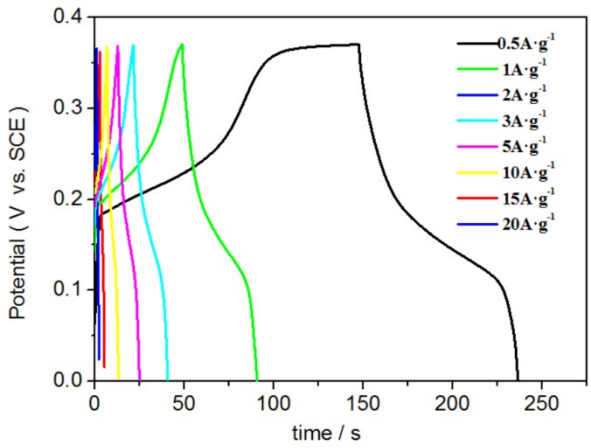

Figure S12. The galvanostatic charge-discharge curves of **3** electrodes at current densities of 0.5-20 A g^{-1} in 6 M potassium hydroxide aqueous solution.

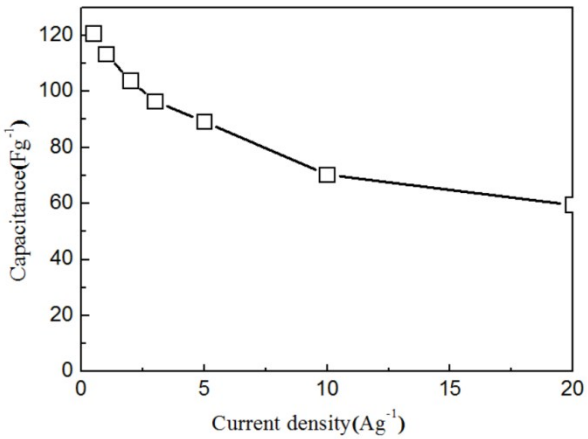

Figure S13. Specific capacitances of **1** and **2** electrodes derived from the discharging curves at the current density of 0.5-20 A g^{-1} in 6 M potassium hydroxide aqueous solution.